Optimization design of the hydro-pneumatic suspension system for high clearance self-propelled sprayer using improved MOPSO algorithm

Fan Yang[1,2], Yuefeng Du[1,2], Changkai Wen[1,2], Zhen Li[1,2], Enrong Mao[1,2*], Zhongxiang Zhu[1,2]

(1. *College of Engineering, China Agricultural University, Beijing 100083, China*;
2. *Beijing Key Laboratory of Optimized Design for Modern Agricultural Equipment, China Agricultural University, Beijing 100083, China*)

Abstract: Large high clearance self-propelled sprayers were widely used in field plant protection due to their high-efficiency operation capabilities. Influenced by the characteristics of field operations such as high power, heavy weight, high ground clearance, and fast operation speed, the comprehensive requirements for the ride comfort, handling stability and road friendliness of the sprayer were increasingly strong. At the present stage, the chassis structure of the high clearance self-propelled sprayer that attaches great importance to the improvement of comprehensive performance still has the problems of severe bumps, weak handling performance and serious road damage in complex field environments. Therefore, this paper proposes an optimization design method for hydro-pneumatic suspension system of a high clearance self-propelled sprayer based on the improved MOPSO (Multi-Objective Particle Swarm Optimization) algorithm, covering the entire process of configuration design, parameter intelligent optimization, and system verification of the high clearance self-propelled sprayer chassis. Specifically, chassis structure of the hydro-pneumatic suspension suitable for the high clearance self-propelled sprayer was designed, and a design method combining the improved MOPSO algorithm based on time-varying fusion strategy and adaptive update with the parameter optimization of hydro-pneumatic suspension based on this algorithm was proposed, and finally the software simulation and bench performance verification were carried out. The results show that the optimized hydro-pneumatic suspension has excellent vibration reduction effect, and the body acceleration, suspension dynamic deflection and tire deflection were increased by 16.5%, 9.9% and 0.9% respectively, compared with those before optimization. The comprehensive performance of the hydro-pneumatic suspension designed in this study is better than that of the traditional suspension.

Keywords: high clearance self-propelled sprayer, vibration reduction, hydro-pneumatic suspension, MOPSO, multi-objective optimization

DOI: 10.25165/j.ijabe.20241702.7813

Citation: Yang F, Du Y F, Wen C K, Li Z, Mao E R, Zhu Z X. Optimization design of the hydro-pneumatic suspension system for high clearance self-propelled sprayer using improved MOPSO algorithm. Int J Agric & Biol Eng, 2024; 17(2): 109–122.

1 Introduction

As a large-scale high-end agricultural equipment, the large high clearance sprayer is widely used in the stage of crop spraying and fertilization[1-4]. Compared with the non road vehicles such as military vehicles and engineering vehicles[5,6], the complex field working environment when large high sprayers operate at high speeds puts forward higher requirements for their suspension and vibration reduction systems[7,8]: 1) Ensure that the structure is highly integrated to reduce crop damage; 2) Improve the ride comfort and handling stability of field operation; 3) Relieve soil compaction caused by heavy weight and improve road friendliness; (4) Ability to adjust chassis height according to crop height.

The traditional air spring passive suspension system can realize the functions of vibration reduction and small-scale chassis adjustment[9]. However, in the face of complex conditions such as field potholes, crop plant protection with different plant heights and multi-level road driving, due to its own structure, it is unable to achieve high-performance vibration reduction and large-scale chassis clearance adjustment, and the comfort and handling performance are not good, which has a great impact on the spray stability of the boom[10,11]. The hydro-pneumatic suspension benefits from the advantages of hydraulic cylinder with accumulator for vibration reduction, large-scale damping adjustment of hydraulic system and compact structure layout, which can achieve improved vibration reduction performance and wider range chassis height adjustment function[12-14], it has certain advantages in solving the problem of reducing vibration of sprayers, and has broad application prospects. However, with the complexity of the hydraulic system and the high integration of the hydro-pneumatic suspension structure, there are many parameters that affect the vibration reduction effect, and the complex combination of parameters has a significant nonlinear impact on the suspension performance[15]. These problems make it difficult to clarify the relationship between the vibration reduction performance and the inherent characteristics of the suspension, and make the influence of the multi-parameter coupling in the hydro-pneumatic suspension structure on the nonlinear system become increasingly serious. Therefore, it is increasingly difficult to establish a set of structure

Received date: 2022-07-19 **Accepted date:** 2023-11-20

Biographies: Fan Yang, PhD, research interest: off-road vehicle design and dynamics analysis, Email: yf1762773980@163.com; **Yuefeng Du**, PhD, Associate Professor, research interest: digital twin of agricultural equipment, Email: dyf@cau.edu.cn; **Changkai Wen**, PhD, research interest: intelligent technology of agricultural equipment, Email: 18813003909@163.com; **Zhen Li**, Associate Professor, research interest: intelligent sensing and control technology for agricultural equipment, Email: zhenli@cau.edu.cn; **Zhongxiang Zhu**, Professor, research interest: vehicle system dynamics, Email: zhuzhonxiang@cau.edu.cn.

***Corresponding author: Enrong Mao**, PhD, Professor, research interest: vehicle electronic control and intelligent technology. College of Engineering, China Agricultural University, Beijing 100083, China. Tel: +86-13501288688, Email: gxy15@cau.edu.cn.

and model suitable for the vibration reduction system of high clearance self-propelled sprayer.

Many researchers have carried out a lot of research and experiments on the optimization analysis of suspension system characteristics. Solomon et al.[16] analyzed the impact trend of stiffness and damping characteristics on the smoothness of tracked vehicle hydro-pneumatic suspensions. Gundogdu[17] established a dynamic model based on damping and stiffness, designed the dimensionless expressions of head acceleration, peak factor, suspension dynamic deflection and tire deflection, and optimized the quarter car seat suspension. Gobbi et al.[18] adopted a two-degree-of-freedom model to describe the dynamic behavior of road driving, and improved the vehicle's grip and working space by optimizing the stiffness and damping of passive suspension. Peng et al.[19] used the GA-PSO algorithm to improve the damping and stiffness of the tires and suspension of off-road vehicles, in order to achieve the best damping performance. Kuznetsov et al.[20] established a dynamic model that couples stiffness and damping with the driver, vehicle body, and road surface, and used the Global Optimization Problem Algorithm (AGOP) to optimize ride comfort. In the above suspension design and analysis, some people design the suspension system by establishing the hydraulic system model without considering the suspension dynamic characteristics, while others establish the dynamic model through Newton's law, and analyze the stiffness and damping coefficient to improve the suspension characteristics, but the stiffness and damping coefficient are time-varying in actual operation, so that the suspension characteristic analysis only exists in theoretical research, and the optimization of the suspension is difficult to be applied. It is very rare to truly start with the hydraulic system, analyze its nonlinear characteristics fundamentally, and conduct comprehensive optimization of structural parameters. Therefore, starting from the oil system, establishing a mathematical model with complex structural parameters as input and analyzing the spray hydro-pneumatic suspension accurately is the priority among priorities in the optimization of ride comfort, handling stability and road friendliness.

Multi-objective optimization algorithm is widely used in solving the internal conflict of multi-objective and realizing the compromise of multi-objective[21]. In the fields of military vehicles and engineering vehicles, some researchers have carried out relevant research on suspension optimization by using multi-objective algorithm. Farid et al.[22] established a quarter vehicle model, used genetic algorithms to analyze head acceleration and seat shaking, and optimized vehicle vibration reduction performance. Wu et al.[23] established a rigid-flexible coupling model to improve the efficiency of model analysis, and used ISIGHT to optimize the contradictory relationship between vehicle handling and driving characteristics. Mohsen et al.[24] aiming at the problem of poor vibration reduction effect of military armored vehicle suspension, took ride comfort and driving performance as optimization goals, and proposed an optimal vibration reduction scheme for military armored vehicles through genetic algorithm. Gomes et al.[25] used the PSO algorithm to evaluate the variance of road load and suspension displacement, and used this to analyze the minimization of the objective function. The above optimization provides a reference for the multi-objective optimization of the sprayer's hydro-pneumatic suspension, but the performance indicators of most suspension optimizations are simple, which are not enough to cope with the complex field operation environment faced by the sprayer's vibration reduction. At the same time, existing algorithms cannot balance global and local optima in the face of extremely complex nonlinear hydraulic models, losing the necessity of using algorithms for optimization.

Based on this, in order to meet the complex vibration reduction requirements of high clearance self-propelled sprayers in farm working conditions, in view of the serious bumps, weak handling performance and serious road damage in the chassis system, this study establishes a chassis design, structural optimization and system verification method suitable for high clearance self-propelled sprayers. The main work contents include: 1) By introducing the hydro-pneumatic suspension system and the parallel structure of the damping holes, an innovative configuration based on the hydro-pneumatic suspension chassis of the high clearance self-propelled sprayer is proposed; 2) An optimization method for the structural parameters of the hydro-pneumatic suspension based on the time-varying fusion algorithm is proposed; 3) The algorithm verification and system optimization verification methods are constructed, and a performance test bench is built for verification.

2 Material and methods

2.1 Configuration and analysis of hydro-pneumatic suspension

2.1.1 Hydro-pneumatic suspension configuration

(1) Structure and working principle of hydro-pneumatic suspension

Aiming at the problems that the traditional air suspension in field operation has limited vibration reduction and cannot adjust the ground clearance greatly, an hydro-pneumatic suspension system for sprayer working conditions is proposed. In this paper, combined with the basic parameters and functional requirements of the self-developed 3WPG-3000 high clearance self-propelled sprayer, the designed sprayer's hydro-pneumatic suspension chassis structure is shown in Figure 1. When the sprayer is transported on the asphalt pavement, the hydraulic cylinder 3 is retracted to reduce the center of gravity and improve the handling stability. When the sprayer works in the field, the hydraulic cylinder 3 adjusts the chassis height in real time according to the crop height, so as to avoid damaging crops. The guide mechanism 4 slides in the bearing with the movement of the hydraulic cylinder to realize the guiding function and transfer the steering torque. Compared with the traditional air suspension, the structure of the hydro-pneumatic suspension system is placed under the vertical shaft, and the design is compact, reducing the interference of crops and improving the mobility of sprayer.

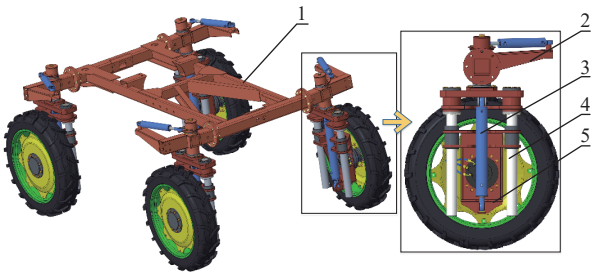

1. Frame 2. Steering System 3. Hydraulic Cylinder 4. Guiding Mechanism 5. Hydro. pneumatic Suspension Fixing Mechanism Tires and Motors

Figure 1 Design of sprayer hydro-pneumatic suspension chassis

(2) Key component design and parameter analysis

1) Steering system design

The steering mechanism of the high ground clearance sprayer conforms to the basic theory of trapezoidal four-link steering[26], but the structure is different from the traditional four-link mechanism, so it is difficult to optimize the sprayer steering system by using the

trapezoidal four-link theory. In this paper, the steering cylinder is regarded as the tie rod of the trapezoidal four-bar linkage, and the equivalent structure is shown in Figure 2.

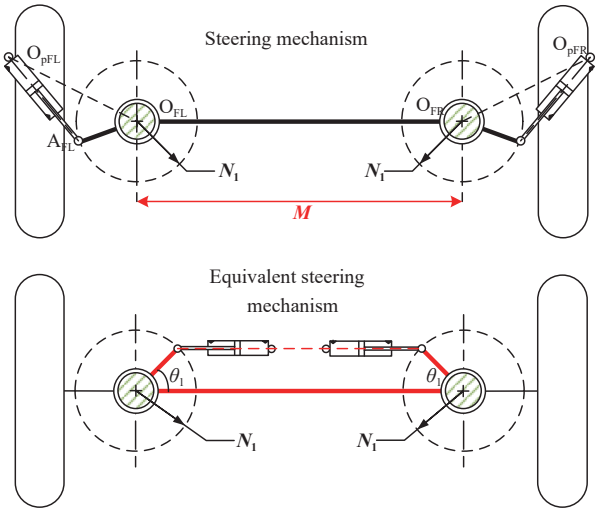

Figure 2 Equivalent trapezoidal four-link

When the high clearance self-propelled sprayer is turning, the steering trapezoid should make the steering wheels of the inner and outer sides roll along the different corners of the same center. The theoretical corner of the Ackerman steering principle is used as the design standard, and the relationship between the actual rotation angle of the inner and outer steering wheels meets the Equation (1).

$$\alpha' = \arctan\frac{N_1\sin(\theta_1-\beta')}{M-N_1\cos(\theta_1-\beta')}-\theta_1+\arccos\frac{[N_1+2M\cos\theta_1-2N_1\cos^2\theta_1-M\cos(\theta_1-\beta')]}{\sqrt{N_1^2+M^2-2N_1M\cos(\theta_1-\beta')}} \quad (1)$$

where, α' and β' are the actual rotation angles of the outer and inner wheels, (°); M is the distance between the main pins, mm; N_1 is the length of the steering arm, mm; θ_1 is the bottom angle of the steering trapezoid. During optimization, the steering trapezoid arm is limited to 150-300 mm and the bottom angle of the steering trapezoid is 65°-75°, the minimum difference between the actual rotation angle of the outer steering wheel and the theoretical rotation angle is taken as the optimization target, that is,

$$f = \min|\alpha-\alpha'| < 3^\circ \quad (2)$$

Before the steering mechanism is optimized, in order to avoid the "dead point" caused by the too small angle between the steering trapezoid arm and the oil cylinder, the minimum transmission angle ξ is established as the constraint condition, namely

$$\xi = \arccos\frac{-M\cos(\theta_1+\delta_{max})+2M\cos\theta_1-2N_1\cos^2\theta_1}{M-2N_1\cos\theta_1} > 30^\circ \quad (3)$$

where, δ_{max} is the maximum actual outer wheel angle, (°). The Matlab R2020b analysis shows that: after optimization, the bottom angle of the steering trapezoid is 69.55°, the length of the steering arm is 160 mm, and the maximum actual outer wheel angle is 28.02°. As shown in Figure 3, the difference between the optimized turning angle and Ackerman's theoretical turning angle is 0.64°, and the steering performance is better than that before the optimization, which can effectively avoid abnormal wear of the steering wheel.

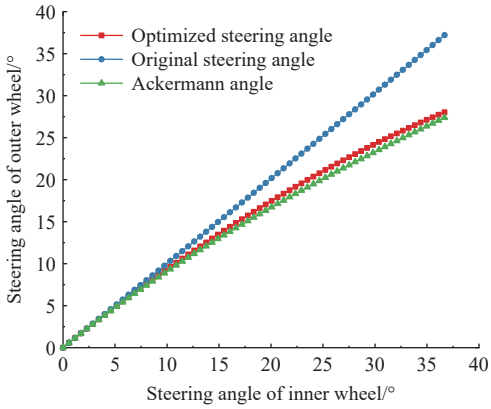

Figure 3 Comparison of internal and external corners before and after optimization

2) Handling performance analysis

Due to the complex operating environment of the sprayer, the characteristics of high ground clearance put forward higher requirements on the driving ability of the sprayer. In this section, force analysis is carried out under the conditions of sprayer braking and climbing to verify the handling performance of the new chassis structure.

As shown in Figure 4, when the sprayer brakes in an emergency, the front axle is subjected to both vertical load and inertial force, and the vertical load moves to the front axle, that is,

$$G_{b1}\frac{L}{2} = G_{b2}\frac{L}{2} + F_{b1}h + F_{b2}h \quad (4)$$

where, G_{b1} and G_{b2} are the reaction forces of the road surface to the front and rear wheels, N; F_{b1} and F_{b2} are the braking forces of the front and rear wheels, N. Since the braking force is equal to the product of the peak adhesion coefficient φ and the reaction force of the road surface, the reaction force of the road surface is equal to the sum of the sprung mass of the single wheel and the inertial force, which can be obtained:

$$\begin{cases} G_{b1} = \left(\frac{1}{2}+\frac{\varphi h}{H}\right)G_m \\ G_{b2} = \left(\frac{1}{2}-\frac{\varphi h}{H}\right)G_m \end{cases}$$

When the sprayer is climbing, the mass of the whole vehicle moves backward, and the ground reaction forces of the front and rear wheels G_{p1} and G_{p2} can be obtained when the slope is θ, as shown in Equation (5).

$$\begin{cases} G_{p1} = \left(\frac{\cos\theta}{2}-\frac{h}{H}\sin\theta\right)G_m \\ G_{p2} = \left(\frac{\cos\theta}{2}+\frac{h}{H}\sin\theta\right)G_m \end{cases} \quad (5)$$

Compared with the upper air suspension structure, the lower hydro-pneumatic suspension structure can effectively reduce the height of the center of gravity h.

3) Hydro-pneumatic suspension chassis design

Combined with the operation requirements, the ground gap adjustment function is designed to make the chassis system realize the adjustment function of 1.5-2.1 m, as shown in Figure 5.

The offset distance of the vertical axle is the distance between the extension line of the steering vertical axle and the contact point between the wheel center and the ground, which is used to maintain the stability of straight driving[27]. The offset distance is positive when the intersection of the extension line is located on the inside of the tire, and the vertical axis offset distance of the sprayer is

usually set to a positive value to ensure that the steering is light. Based on the design principle that the offset distance is positive when the ground clearance is the highest and the lowest, the inclination angle of the vertical axis is set to 3°, and the corresponding offset distance is 187.2-218.6 mm.

After the strength check, the chassis structure parameters are listed in Table 1.

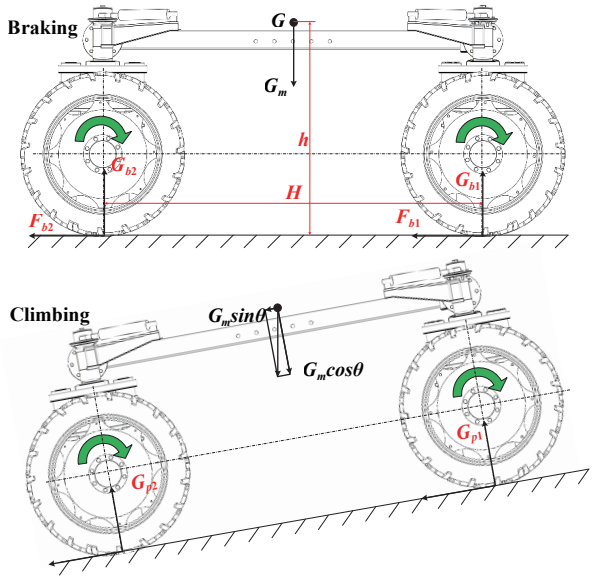

Figure 4 Schematic diagram of climbing and braking conditions

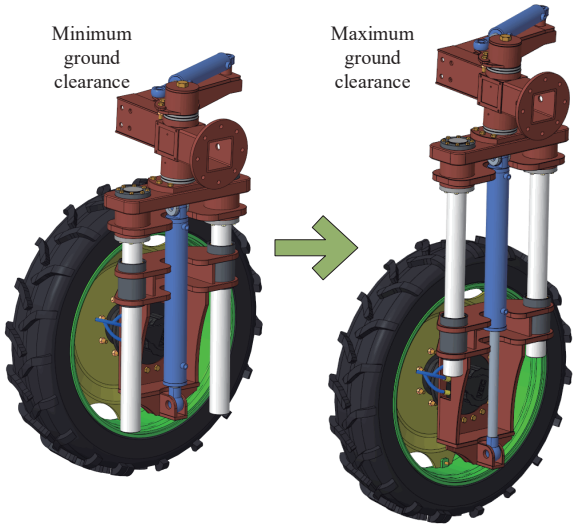

Figure 5 Schematic diagram of ground clearance adjustment

Table 1 Design parameters of chassis.

Parameter symbol	Explanation	Numerical value
m/kg	Total weight	11 480
m_s/kg	Sprung mass of single wheel	2400
m_u/kg	Unsprung mass of single wheel	470
S/mm	Hydraulic cylinder stroke	600
D_x/mm	Diameter of guide column	90
D_l/mm	Diameter of vertical shaft	120

(3) Oil circuit system design

In order to adapt to the complicated and changeable conditions of the sprayer, aiming at the problem of low variable threshold of damping and stiffness of traditional suspension, a hydro-pneumatic spring oil circuit system with parallel structure of damping holes is proposed to improve the damping time-varying range, and the 1/4 suspension model of sprayer is set up, as shown in Figure 6.

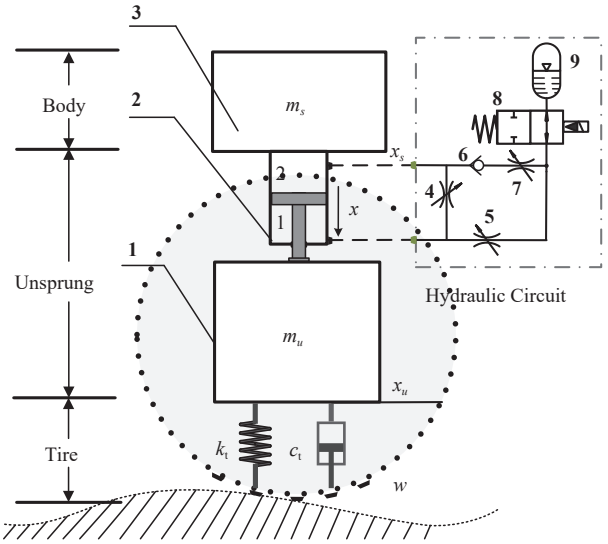

1. Unsprung mass 2. Hydraulic cylinder 3. Body mass 4. Damping hole 5. Damping hole 6. Check valve 7. Damping hole 8. Solenoid on. off valve 9. Accumulator

Figure 6 Hydro-pneumatic suspension model

The suspension model is composed of tire model, unsprung model, body model and hydro-pneumatic suspension system. The tire model is composed of linear spring and linear damper. During the working process, the solenoid on-off valve 8 is normally open. When the body moves upward, part of the hydraulic oil in the rod cavity flows through the damping hole 4 and enters the rodless cavity, and the other part flows through the damping hole 5 and enters the accumulator 9; When the body moves downward, part of the hydraulic oil in the rodless cavity flows through the damping hole 4 into the rod cavity, and the other part enters the accumulator 9 through the check valve 6 and the damping hole 7. When the hydraulic cylinder is compressed, check valve 6 opens and hydraulic oil passes through damping holes 4, 5, and 7. At this point, the function is equivalent to the spring of a traditional suspension; When the hydraulic cylinder is extended, check valve 6 closes and hydraulic oil only flows through damping holes 4 and 5. At this point, the flow rate is relatively high, acting like a damper in traditional suspension. The innovation of this structure lies in the hydraulic oil circuit with parallel damping hole structure. Compared with the hydro-pneumatic suspension system of engineering vehicles, this system innovatively adds check valve 6 and damping hole 7. Since the damping force has the characteristics of time-varying with the excitation amplitude of the road surface, the structure increases the damping threshold of the hydro-pneumatic suspension and better adapts to the comprehensive vibration reduction requirements of high clearance self-propelled sprayers.

After calculation, the structural parameters of the designed oil circuit system are listed in Table 2.

2.1.2 Nonlinear characteristic analysis

The structure designed above covers the accumulator, damping valve, hydraulic cylinder and other components, which promotes the establishment of mathematical model and the improvement of the performance of the whole machine. Traditional nonlinear analysis mostly considers the relationship between stiffness, damping and dynamic model. To accurately establish a mathematical model and analyze the influencing factors of

suspension in an all-round way, the performance components such as accumulator, damping valve, and hydraulic cylinder cannot be ignored. Therefore, by establishing the mathematical model of the damping hole parallel system proposed in this paper, the coupling relationship between the oil circuit system and the dynamics is quantified.

Table 2 Design parameters of oil circuit

Parameter	Explanation	Numerical value
d_1/mm	Piston rod diameter	35
d_2/mm	Hydraulic cylinder inner diameter	63
d_z/mm	Diameter of damping hole 4	4
d_j/mm	Diameter of damping hole 5 and 7	4
P_0/MPa	Initial pressure of accumulator	12
V_0/L	Accumulator charging volume	2.5

(1) Mathematical model of hydro-pneumatic suspension

According to the above model, when the hydraulic cylinder is working, the output force of the hydro-pneumatic suspension is equal to the sum of the elastic force and the damping force, namely

$$F = p_2A_2 - p_1A_1 = k_s(x_s - x_u) + c_s(\dot{x}_s - \dot{x}_u) \tag{6}$$

where, p_1 and p_2 are the pressure of rod cavity and rodless cavity, Pa; x_s and x_u are the body displacement and unsprung displacement, m; k_s is the stiffness coefficient of hydro-pneumatic suspension, N/m; c_s is the damping coefficient of hydro-pneumatic suspension, N·s/m; A_1 and A_2 are the effective area of the rod cavity and the rodless cavity, m^2.

Due to the nonlinear characteristics of the hydraulic system, the stiffness coefficient and damping coefficient of the hydro-pneumatic suspension cannot be determined. The inherent parameters of the suspension are introduced into the model, and the following preconditions are set: 1) Ignore friction and leakage; 2) Assume that the gas is an ideal gas; 3) Ignore external disturbances; 4) Assume that the temperature of the working medium is constant, according to the ideal gas equation of state, the elastic force output by the hydro-pneumatic suspension is obtained as:

$$F_k = p(A_2 - A_1) = \frac{P_0V_0^r(A_2 - A_1)}{[V_0 - (A_2 - A_1)X]^r} \tag{7}$$

where, p and p_0 are the accumulator pressures in the working state and initial state; V and V_0 are the accumulator gas volume in the working state and initial state, and r is the gas variability index.

The damping hole 4 is set as a thick wall orifice, and the damping holes 5 and 7 are set as slender orifices to obtain the flow through the damping hole.

$$\begin{cases} q_z = C_qA_z\sqrt{2\dfrac{\Delta p_1}{\rho}} \\ q_i = \dfrac{\pi d_j^4}{128\mu L}\Delta p_2 \\ q_j = \dfrac{\pi d_j^4}{128\mu L}\Delta p_3 \end{cases} \tag{8}$$

where, q_z, q_i and q_j are the flows of damping holes 4, 5 and 7 respectively, m^3/s; C_q is the orifice flow coefficient, recorded as 0.82; μ is the dynamic viscosity of hydraulic oil, Pa·s; L is the overflow length of throttle orifice, m. According to the working principle of parallel damping hole oil circuit analyzed above, the working process of suspension can be expressed by Equation (9).

$$\begin{cases} A_1\dot{X} = \text{sign}(\dot{X})q_z + q_i \\ (A_2 - A_1)\dot{X} = \left[\dfrac{1}{2} + \dfrac{1}{2}\text{sign}(\dot{X})\right]q_j - q_i \end{cases} \tag{9}$$

The damping force obtained by sorting is shown in Equation (10).

$$F_c = \frac{\rho A_2^3\dot{X}^2\text{sign}(\dot{X})}{2\left[C_qA_z + \dfrac{\pi d_j^4}{128\mu L}\left(\dfrac{1}{2} + \dfrac{1}{2}\text{sign}(\dot{X})\right)\right]^2} + \frac{128\mu LA_1(A_2 + A_1)\dot{X}}{\pi d_j^4} \tag{10}$$

Calculate the partial derivative of Equation (7) and (10), and the expressions of stiffness coefficient and damping coefficient are:

$$k_s(x) = \frac{rP_0V_0^r(A_2 - A_1)^2}{[V_0 - (A_2 - A_1)x]^{r+1}} \tag{11}$$

$$c_s(\dot{x}) = \frac{\rho A_2^3\dot{x}\text{sign}(\dot{x})}{\left[C_qA_z + \dfrac{\pi d_j^4}{128\mu L}\left(\dfrac{1}{2} + \dfrac{1}{2}\text{sign}(\dot{x})\right)\right]^2} + \frac{128\mu LA_1(A_2 + A_1)}{\pi d_j^4} \tag{12}$$

The nonlinear vibration model of hydro-pneumatic suspension can be obtained by Newton's law of motion, as shown in Equation (13).

$$\begin{cases} m_s\ddot{x}_s = -k_s(x_s - x_u) - c_s(\dot{x}_s - \dot{x}_u) \\ m_u\ddot{x}_u = k_s(x_s - x_u) + c_s(\dot{x}_s - \dot{x}_u) - k_t(x_u - w) - c_t(\dot{x}_u - \dot{w}) \end{cases} \tag{13}$$

where, m_s and m_u are sprung mass and unsprung mass; w is the input displacement of pavement; k_t and c_t are the stiffness coefficient and damping coefficient of the tire. Combining Equations (11) and (12), the stiffness coefficient and damping coefficient in the dynamic model can be replaced by the hydraulic system model, which is convenient to establish the nonlinear coupling model below.

(2) Nonlinear characteristic analysis of hydro-pneumatic suspension

The analysis of the damping characteristics of hydro-pneumatic suspension is complex. In order to comprehensively determine the performance parameters that affect the sprayer's hydro-pneumatic suspension, the nonlinear characteristics of hydro-pneumatic suspension are analyzed based on the oil circuit model.

According to Equations (7) and (10), the initial pressure of the accumulator, the charging volume of the accumulator, the effective action area of the hydraulic cylinder and the diameter of the damping hole are the key parameters affecting the output force of the suspension. Therefore, single factor analysis is conducted for the above parameters. Under the sinusoidal signal with amplitude of 0.05 m and excitation frequency of 3 Hz, adjust the initial pressure of accumulator P_0, inflation volume V_0, inner diameter of hydraulic cylinder d_2, piston rod diameter d_1, damping hole diameter d_z and d_j, and analyze the nonlinear characteristics of suspension. The change trend of elastic force and damping force is shown in Figure 7.

It can be seen from Figure 7a that within a certain range of hydraulic cylinder action, except for the accumulator charging pressure that has been determined at the beginning of the sprayer design, the charging volume and the diameter of the piston rod have a greater impact on the elastic force of the hydro-pneumatic suspension. It can be seen from Figure 7b that the damping force has a great correlation with the damping hole and the inner diameter of the hydraulic cylinder. The change curve of the hydraulic cylinder inner diameter in Figure 7a is coincident, and the curve of the piston rod diameter in Figure 7b is also coincident. To sum up, it

can be seen that the accumulator charging volume, piston rod diameter, damping hole diameter and hydraulic cylinder inner diameter are important parameters for optimizing the performance of the hydro-pneumatic suspension.

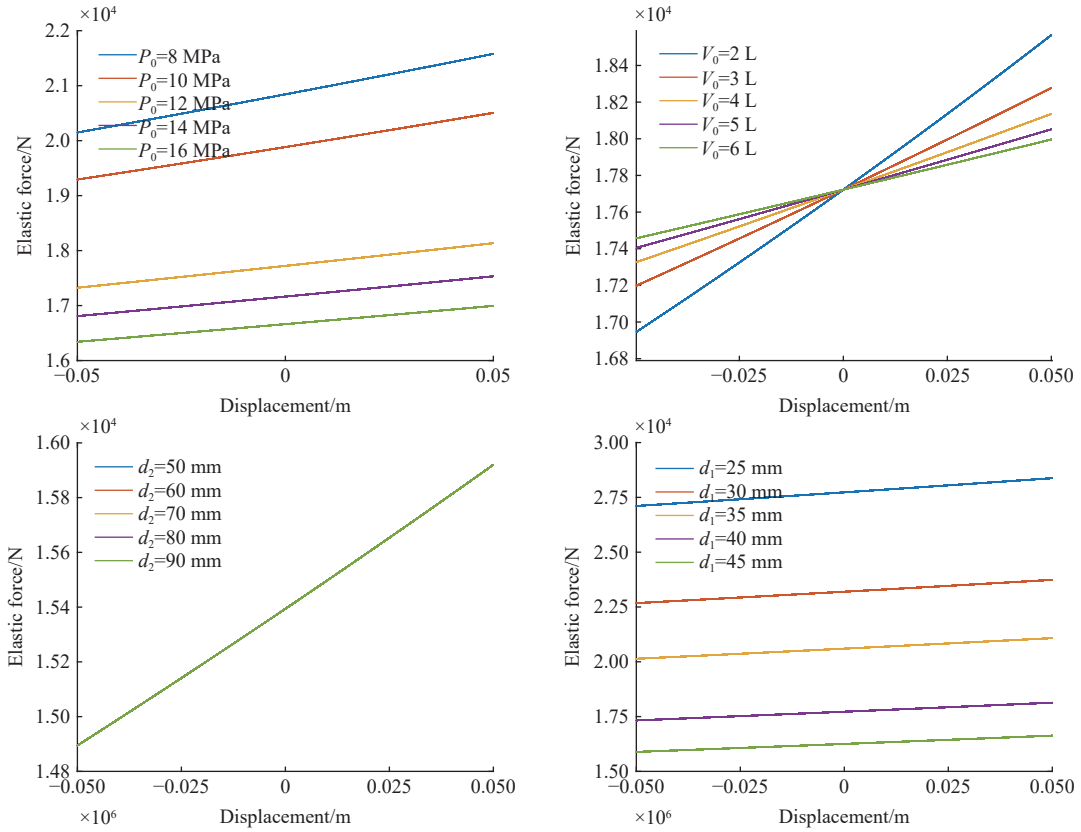

a. Change trend of elastic force

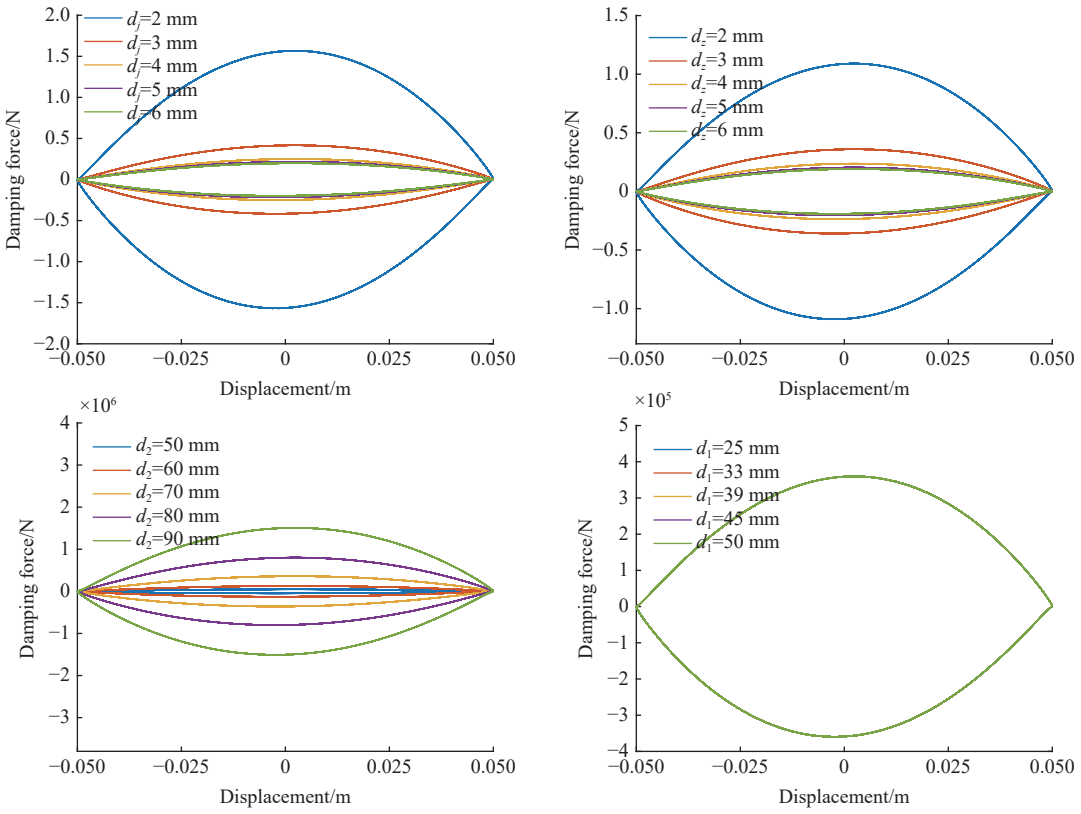

b. Change trend of damping force

Figure 7 Relationship between suspension characteristics with parameters

2.2 Intelligent optimization of parameters

The system design index is based on static performance and does not take into account the complexity and related influence of dynamic operation process. Therefore, it is one of the focuses of this

study to explore the intelligent optimization method of parameters affecting the sprayer's hydro-pneumatic suspension.

2.2.1 Improved MOPSO algorithm based on time-varying fusion method

As one of the classic multi-objective optimization algorithms, the MOPSO algorithm integrates the characteristics of the PSO algorithm, and is widely used in power grid capacity scheduling, water resource scheduling and other fields[28]. However, each particle in the traditional MOPSO algorithm has a unintelligent flight speed and direction. As shown in Figure 8, particle swarm optimization algorithm searches for the optimal solution in space by following the current global optimal particle and individual optimal particle.

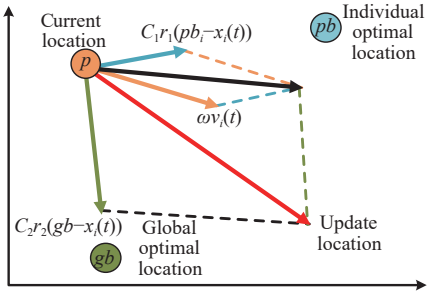

Figure 8 Schematic diagram of particle motion

According to the analysis of Figure 8, the particle motion direction is affected by three factors: 1) Inertial motion according to its own velocity; 2) According to the particle cognition during iteration, approach to the optimal position of the individual; 3) Through information exchange, search the current optimal particle and move to the global optimal. Suppose that each particle is initialized in the j-dimensional space, and the particle position and velocity are represented by $x_i=(x_{i1}, \ldots, x_{ij})$ and $v_i=(v_{i1}, \ldots, v_{ij})$.

$$v_i(t+1)=\omega v_i(t)+c_1r_1(pb_i-x_i(t))+c_2r_2(gb-x_i(t)) \tag{14}$$

$$x_i(t+1)=x_i(t)+v_i(t+1) \tag{15}$$

where, t is the current number of iterations; ω is the inertia weight of PSO, when ω is large, the algorithm has strong global search ability, and when ω is small, the algorithm has strong local search ability; c_1 and c_2 are the individual learning factor and the social learning factor, respectively. r_1 and r_2 are random numbers in the interval (0,1); pb_i is the optimal solution of individual i, and gb is the global optimal solution of the current iteration.

Specifically, when ω is too large, the particle is greatly affected by the inertial force and move in the direction of its own motion, the convergence speed of the algorithm is too slow and the purpose of the search is insufficient; When ω is too small, the particle is less affected by its own inertia, and more moves to the current optimal particle, and the effect is not good. The individual learning factor c_1 represents the particle's self-learning ability. When c_1=0, the particle is only affected by the current "optimal" c_2, and the convergence speed is faster, but it is difficult to find the global optimum when solving complex problems; The social learning factor c_2 determines the social information sharing ability of particles. When c_2 = 0, particles will not approach the current global optimum, and the search effect is poor only through the "self cognition" factor c_1.

The traditional MOPSO algorithm uses the fixed inertia weight to balance the global and local search, which makes it have poor convergence and easy to fall into local optimization when dealing with complex calculation models[29]. It is difficult to converge to Pareto front when optimizing the suspension coupling mathematical model with strong nonlinear characteristics.

Therefore, aiming at the fixity of particle velocity direction and position updating, Therefore, aiming at the fixity of particle velocity direction and position update, this paper proposes a method of multiple time-varying factors and real-time dynamic updating particles. It includes the particle velocity of time-varying fusion strategy and adaptive updated particle position. On the issue of particle velocity, the original inertia weight is changed into time-varying weight, and a factor fusion strategy is proposed to solve the defect of single particle flight direction and realize the real-time adjustment effect of particle flight direction. On the issue of particle position update, the problem that the particle position can only be changed through the velocity direction is solved by introducing adaptive weight factor, so as to realize the dynamic update of particle position and intelligently balance the relationship between global and local search.

(1) Particle velocity of time-varying fusion strategy

By comparing the pros and cons of the father and son generations to judge whether evolution has occurred, the probability of not evolving $Ps(i)$ is

$$P_s(t)=\frac{\sum_{i=1}^{N}Q(i,t)}{N} \tag{16}$$

where, when pb_{i-1} is better than pb_i, $Q(i,t)$ is recorded as 1, otherwise it is 0; N is the total number of particles and i is the current particle. When the probability value is large, it indicates that the number of non-dominated solutions in the last iteration is small. Therefore, the inertia weight is adjusted in real time according to the probability value to adaptively improve the global search ability. In the later stage of the iteration, most of the non-dominated solutions are close to the Pareto frontal surface, which adaptively reduces the global search ability, improves the local search ability, and makes the algorithm converge quickly. From this principle, the inertia weight ω_1 is obtained as Equation (17).

$$\omega_1(t)=(\omega_{\max}-\omega_{\min})P_s(t)+\omega_{\min} \tag{17}$$

Among them, $\omega_{\max}$ and $\omega_{\min}$ are taken as 0.9 and 0.4, respectively. In order to make the particles approach the global optimal direction, an inertia weight ω_2 based on the global optimal particle is proposed to supplement ω_1.

$$\omega_2(t)=\omega_{\max}\left(1-\frac{\sqrt{(pb_i-x_i(t))^2+1}}{\sqrt{(gb-x_i(t))^2+(pb_i-x_i(t))^2+1}}\right) \tag{18}$$

With the progress of iteration, the particles should gradually tend to the Pareto front, the particle uniformity is continuously improved, and ω_2 gradually decreases with the iteration, which is in line with this design principle. Thus, the inertia weight ω_1 and ω_2 are fused, and judge the size of inertia weight, and intelligently select the maximum value as the inertia weight of the current iteration.

$$\omega'=\max(\omega_1(t),\omega_2(t)) \tag{19}$$

In the traditional particle swarm optimization algorithm, the values of c_1 and c_2 are usually fixed value 2, which makes the proportion of each factor unchanged in the whole process of the algorithm and can not be adjusted in real time with the actual convergence, Therefore, the learning factors c_1 and c_2 are improved, and the obtained adaptive learning factors are shown in equation (20).

$$c_{1i} = c_{10}\exp\left(\frac{t}{T}\frac{(pb_i - x_i(t))}{\sqrt{(pb_i - x_i(t))^2 + 1}}\right),$$
$$c_{2i} = c_{20}\exp\left(-\frac{t}{T}\frac{(gb - x_i(t))}{\sqrt{(gb - x_i(t))^2 + 1}}\right) \quad (20)$$

In the early stage of iteration, the particle distribution is complex and the location of the optimal solution cannot be determined. The particles should be close to the global optimal particle to quickly approach the Pareto front; In the later stage of iteration, most particles are close to the current global optimum. In order to ensure that the current optimal result does not fall into the local optimum, the evolutionary position of particles should be properly divergent, that is, the proportion of individual optimal direction of particles should be increased to achieve the optimal effect. Therefore, the designed c_{1i} increases with the increase of t and c_{2i} decreases with the increase of t, so as to weigh the proportion of global search and local search.

Finally, the improved particle velocity is shown in the Equation (21).

$$v_i(t+1) = \omega' v_i(t) + c_{1i} r_1 (pb_i - x_i(t)) + c_{2i} r_2 (gb - x_i(t)) \quad (21)$$

(2) Adaptively updated particle position

The traditional position update method is not conducive to the global search. A particle position update method based on adaptive adjustment is proposed. According to the current iteration state, the adaptive factor η is used to change the ratio of $x_i(t)$ and $v_i(t+1)$ in real time, and adjust the weight of global and local search. Therefore, the judgment condition p_i is proposed.

$$p_i = \frac{\exp\left(\frac{1}{N}\sum_{i=1}^{N} x_i(t)\right)}{\exp(x_i(t))} \quad (22)$$

where, p_i is to master the fitness of the current particle by calculating the ratio of the average value of all particles to particle i in the t-th generation. When p_i<1, the current average fitness is better than the fitness of particle i, the search effect of particle i itself is not good, and the global search ability of particle i should be strengthened; When p_i>1, the fitness of particle i is better than the current average fitness, and the overall effect of the current population is poor, particle i should be retained for local search. Therefore, a position update method of adaptive strategy is proposed, which is expressed by Equation (23)

$$x_i(t+1) = \begin{cases} x_i(t) + v_i(t+1), & p_i > 1 \\ \omega_3 x_i(t) + (1-\omega_3) v_i(t+1), & p_i < 1 \end{cases} \quad (23)$$

$$\omega_3 = \omega_{\min} + \frac{(\omega_{\max} + \omega_{\min})t}{T} \quad (24)$$

In principle, the overall fitness in the early stage of the iteration is low, and the algorithm needs to have a strong global search capability. In the later stage of the iteration, most of the particles are close to the Pareto front, which requires higher local search capabilities. Therefore, the weight coefficient ω_3 is proposed to synthesize the proportion of this principle and adaptive location update method. ω_3 increases with the iteration. On the premise of satisfying the adaptive position update, the local search ratio is automatically increased to optimize the iterative effect.

2.2.2 Optimal design method of hydro-pneumatic suspension parameters based on improved algorithm

At present, there are few researches on the optimization design of the suspension system of high clearance self-propelled sprayer. The suspension optimization in other fields mostly focuses on the damping coefficient and stiffness coefficient suspension, but the optimization of stiffness coefficient and damping coefficient can not really map to the actual suspension structure. This paper starts from the working characteristics, and proposes an optimized design method of hydro-pneumatic suspension parameters based on the improved algorithm for the actual structure of hydro-pneumatic suspension, so as to improve the vibration reduction effect of suspension system.

In order to map the nonlinear system to the chassis structure of the high clearance self-propelled sprayer and improve the vibration reduction effect of the system as much as possible, the improved MOPSO algorithm is used to optimize the key design parameters of the suspension of the high clearance self-propelled sprayer. In the face of the hydro-pneumatic suspension with complex nonlinear system and complex parameter coupling, the optimization effect of the traditional algorithm is poor. It is often unable to get close to the Pareto front, and even the "optimal solution set" is concentrated in a certain area, the convergence effect and speed cannot achieve the expected effect, the performance optimization has little effect, and the optimization is not necessary. By integrating multiple time varying factors, the improved algorithm to control the global optimization effect in real time has the advantage of solving the contradiction between global and local search and speeding up the convergence efficiency, which is suitable for the nonlinear mathematical model of hydro-pneumatic suspension. Among them, the speed update method based on time-varying fusion strategy avoids the time consumption of the algorithm in the calculation of poor parameter combination during optimization iteration, and can calculate the optimal parameter combination faster; The updating method of particle position based on adaptive strategy optimizes the relationship between global and local search, and efficiently determines the optimal parameter combination to make it converge faster and reduce the probability of error in the calculation of complex nonlinear system. This method can comprehensively obtain the optimal solution sets of different weights for ride comfort, handling stability and road friendliness, providing more possibilities for the subsequent improvement of sprayer suspension parameters. The algorithm calculation process is shown in Figure 9.

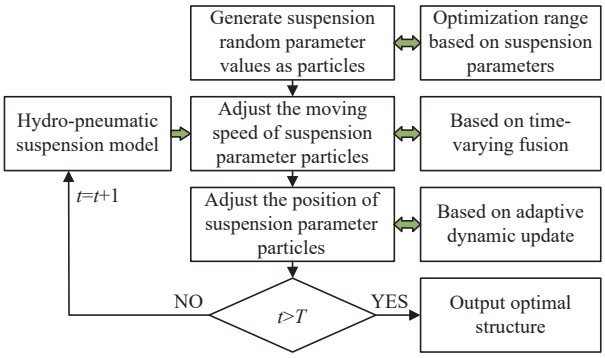

Figure 9 Schematic diagram of improved MOPSO for hydro-pneumatic suspension system

3 System verification

3.1 Software simulation verification

The root mean square of vehicle body acceleration is used to evaluate the ride comfort; The suspension dynamic deflection is used to evaluate the handling stability; The tire deflection

determines the degree of damage to the soil, in order to avoid compacting the soil, it is used to evaluate the road friendliness[30,31].

In order to better reflect the pros and cons of the evaluation indicators, the root mean square of the body acceleration, the root mean square of the suspension dynamic deflection and the root mean square of the tire deflection are used as the objective functions of the algorithm. According to the analysis results of the suspension characteristics in Section 2.1.2, the accumulator charging volume V_0, the hydraulic cylinder inner diameter d_2, the piston rod diameter d_1, and the damping hole diameters d_z and d_j are used as decision variables. By optimizing the decision variables, this paper achieves the best comprehensive effect of ride comfort, handling stability and road friendliness.

According to the intelligent optimization method in Section 2.2.2, the improved algorithm has a good theoretical feasibility for the optimization of the hydro-pneumatic suspension, but due to the complexity of the hydraulic system, an accurate model must be established to reflect the suspension characteristics in the actual optimization. Therefore, this paper does not adopt the traditional method of establishing the objective function, but builds the coupling model of the hydraulic system and the dynamic model in Matlab/Simulink according to the mathematical model established in Section 2.1.2, and establishes the objective function of the improved algorithm on this basis. The structural parameters are used as the model input (Real-time adjustment), and the objective function is used as the model output (Output to algorithm). The assignin and sim function are used to realize the data exchange between the m file of the algorithm and the model I/O, so as to control the coupling model in real time. The coupling model of data exchange is shown in Figure 10.

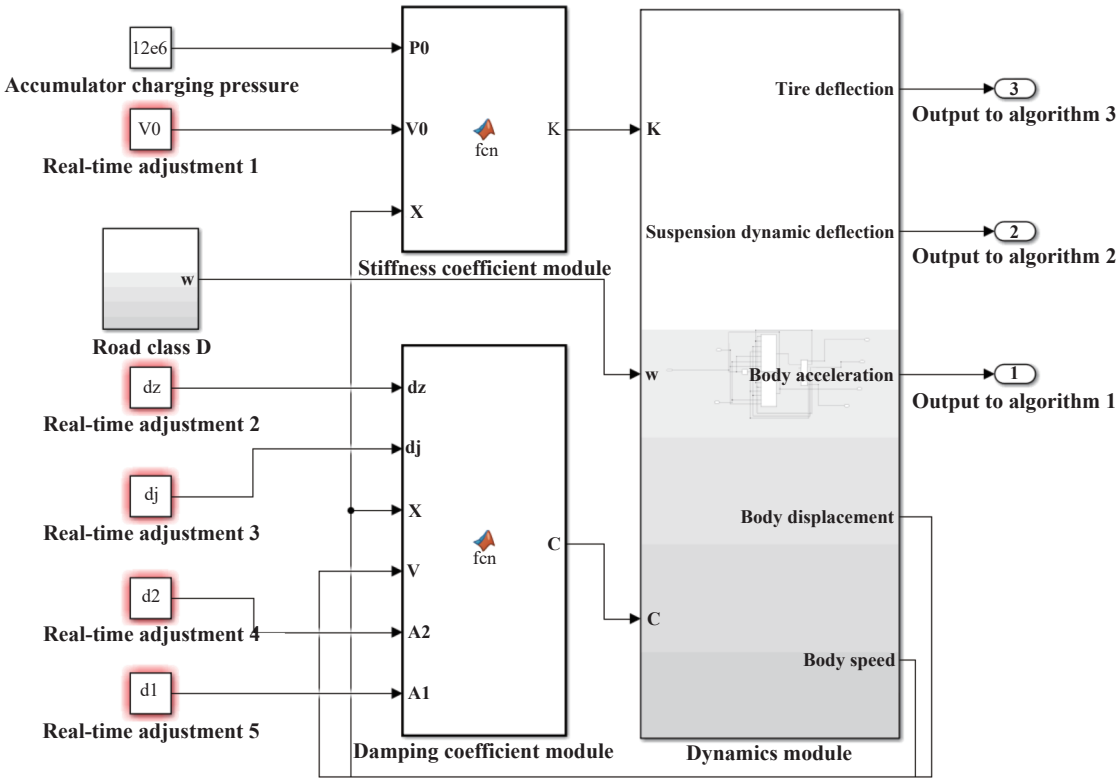

Figure 10 Objective function coupling model

Through calculation and simulation, the feasible range of optimization parameters is defined. Finally, the value range of optimization parameters is listed in Table 3.

Table 3 Optimization range of parameters

Parameters	Lower limit value	Upper limit value
Hydraulic cylinder inner diameter d_2/mm	55	90
Piston rod diameter d_1/mm	20	50
Damping hole 4 diameter d_z/mm	2	9
Damping hole 5, 7 diameter d_j/mm	2	9
Accumulator volume V_0/L	2	7

3.2 Bench performance verification

In order to further explore the optimized suspension performance and verify the superiority of the designed hydro-pneumatic suspension structure, the hydro-pneumatic suspension vibration reduction test bench was built according to the structural parameters of the 3WPG-3000 sprayer, the structure of the test bench is shown in Figure 11. The tire is simulated by a coil spring, and its stiffness coefficient is set to 650 kN/mm, which is the same as the actual tire. The actuator 9 simulates the input of excitation through industrial computer, and the excitation signal is sequentially transmitted to the simulated tire 8, the hydraulic cylinder 7 and the mass block 6 to simulate the vibration reduction process of the sprayer, and the signal received by the sensor is transmitted to the computer in real time. The signal sent by the computer is set to 0.05 m step signal and D-level road signal. The purpose of the 0.05 m step signal test is to verify the correctness of the system characteristic analysis. During the 0.05 m step test, the two ends of the displacement sensor 1 are fixed on the test bench frame and the sprung-loaded position respectively, and the two ends of the displacement sensor 4 are respectively fixed between the actuator and the hydraulic cylinder, which are used to monitor the sprung displacement and the unsprung displacement respectively. During the D-level road test, the acceleration sensor 2 is placed in the spring-loaded position, the two ends of the displacement sensor 3 are fixed on both sides of the hydraulic cylinder 7, and the

displacement sensor 4 is fixed on both ends of the simulated tire 8, which are respectively used to monitor the body acceleration, the suspension dynamic deflection and the tire deflection.

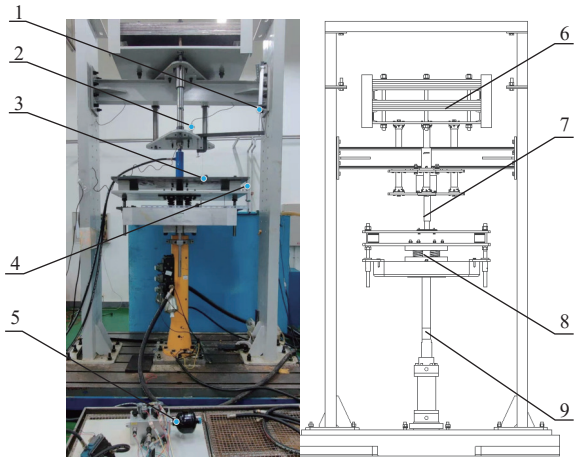

1. Displacement sensor 2. Acceleration sensor 3. Displacement sensor 4. Displacement sensor 5. Hydraulic valve block 6. Mass block simulating body mass 7. Hydraulic cylinder 8. Simulated tire 9. Servo actuator

Figure 11 Hydro-pneumatic suspension vibration test bench

Before the start of the test, two kinds of road input signals are used to test the vibration reduction performance of hydro-pneumatic suspension, and the excitation signal transmission time was set to 10s. The corresponding positions of the test bench were replaced with the suspension structure before and after optimization in turn, and each group was repeated 20 times. After each test, it was allowed to stand for 1 min to avoid the error effect of the increase in oil temperature on the test effect, the sensor data was recorded and the vibration reduction effect was analyzed.

4 Results and discussions

4.1 Algorithm verification results

In this paper, ZDT1, ZDT2, ZDT3 and ZDT6 test functions are used to compare and analyze the algorithms before and after the improvement. In Matlab R2020b, the population size is set to 100, the number of iterations is 1000, and each test is repeated 5 times to take the best one, and the performance evaluation index IGD is used to record the optimization effect in the iterative process[32]. The performance index IGD judges the convergence and distribution performance of the algorithm by calculating the distance between the point on the real Pareto front and the population individuals. The calculation method of IGD is shown in Equation (25).

$$\mathrm{IGD} = \frac{\sum_{i=1}^{N} |d_i|}{N} \tag{25}$$

where, $|N|$ is the number of individual point sets on the real Pareto frontier, and $|d_i|$ is the minimum Euclidean distance between the points on the real front and the current optimal point set. IGD evaluates the overall performance of the algorithm by calculating the average value of the minimum Euclidean distance. When the algorithm has good convergence performance, the corresponding $|d_i|$ is relatively small, which is used to evaluate the convergence of the algorithm. When the algorithm has poor distribution performance, the individuals in the population are relatively concentrated, and most individuals have a large $|d_i|$, otherwise $|d_i|$ is small, this feature is used to evaluate the distribution of the algorithm. The smaller the value of IGD, the better the overall performance of the algorithm, the comparison of algorithm performance before and after improvement is shown in Figure 12 and Table 4.

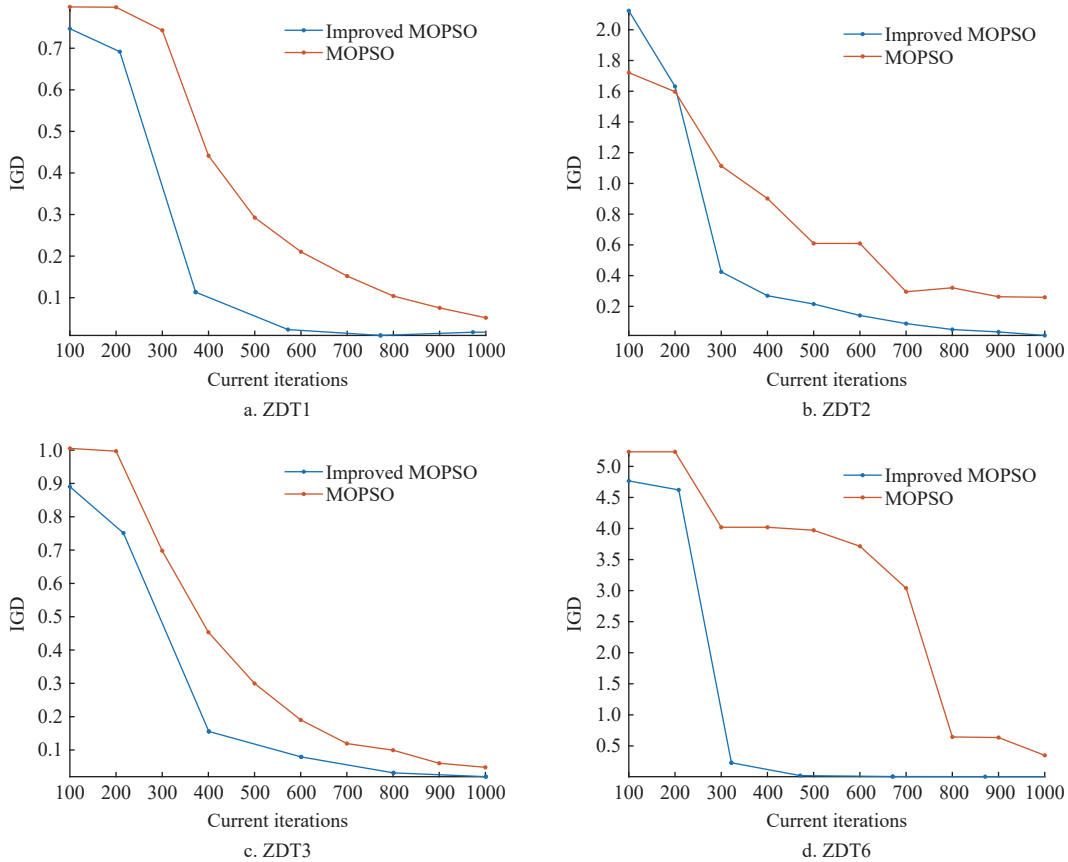

Figure 12 Comparison of the IGD

Table 4 Comparison of the final data of IGD

Function	MOPSO	Improved MOPSO
ZDT1	0.0517	0.0169
ZDT2	0.258	0.011
ZDT3	0.0480	0.0199
ZDT6	0.348	0.05

It can be seen from Figure 12 and Table 4 that the IGD value of the improved MOPSO algorithm is better than that of the MOPSO algorithm in most of the time. The improved algorithm has obvious advantages in the IGD value when the iteration is completed, the convergence speed is faster, and the population distribution is better. Compared with the MOPSO algorithm, the convergence performance and distribution performance of the improved MOPSO algorithm are guaranteed when dealing with complex models. The effectiveness of the improved algorithm is verified by the test function.

4.2 Parameter optimization results

In order to optimize the structure of hydro-pneumatic suspension and explore the performance of the improved algorithm, the classical algorithm NSGA-II in multi-objective optimization is introduced[33,34]. By comparing with the algorithm in this paper, the effect of the improved MOPSO algorithm is analyzed. The coupling model is optimized by NSGA-II algorithm, MOPSO algorithm and improved MOPSO algorithm respectively, the road input signal is set to the D-level road commonly seen in the field. The initial population is set to 200 and the number of iterations is set to 100. The three algorithms are optimized for 5 times each, and the group with the best effect is taken as the result. The optimal solution after suspension parameters optimization is shown in Figure 13.

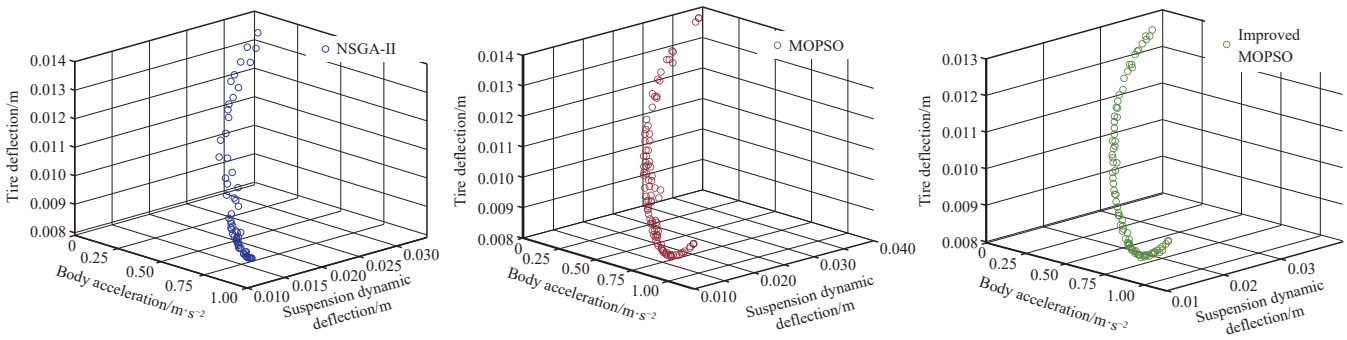

a. NSGA-II b. MOPSO c. Improved MOPSO

Figure 13 Comparison of optimal solution sets

It can be seen from Figure 13 that the NSGA-II algorithm and the MOPSO algorithm have their own characteristics in terms of convergence and population distribution, but when dealing with complex mathematical model of sprayer, the overall optimization effect cannot meet the needs of the optimization of the sprayer's hydro-pneumatic suspension. Since the reason for these two algorithms to participate in the comparison is to verify the advantages of the improved MOPSO algorithm in optimizing the complex mathematical model of the sprayer, the characteristics of the NSGA-II algorithm and the MOPSO algorithm will not be analyzed in detail. Compared with the improved MOPSO algorithm, the particle population distribution in the solution set of the MOPSO algorithm and NSGA-II algorithm is poor, and some particles do not converge to the frontier surface, while the solution set of the improved MOPSO algorithm is smooth, the solution set distribution is more uniform, and it does not fall into the local optimum, and the optimized solution set is closer to the optimization, which verifies the effectiveness of the time-varying fusion strategy in updating the particle velocity and position, improves the practicability and superiority of the algorithm in dealing with complex models, and solves the problem of poor optimization effect of traditional algorithm in dealing with complex coupling models of hydro-pneumatic suspension. The results show that the Pareto front of the improved MOPSO algorithm is superior to the other two algorithms, which proves the superiority of the improved MOPSO algorithm compared with NSGA-II algorithm and MOPSO algorithm.

According to the basic properties of multi-objective optimization, the point set of Pareto front represents the different weights of multiple objectives. Under the complex operating conditions of the sprayer, the ride comfort determines the driver's riding experience and the spraying quality of the boom, and has the highest priority in the performance indicators of vibration reduction; The handling performance of the sprayer directly affects the quality of the field operation, and it is the second priority in the indicators of vibration reduction; Since the increase of tire dynamic load will cause a substantial increase in road damage, the optimization results should ensure that the road friendliness performance of the sprayer cannot deteriorate. Based on this principle, the optimal solution set optimized by the improved algorithm is screened to obtain the optimal combination of evaluation indicators that meet the above principles, and the final parameters are selected according to the mechanical design principles, as listed in Table 5.

Table 5 Comparison of structural parameters before and after algorithm optimization.

Parameter	Original suspension	Optimized suspension	Model selection
Hydraulic cylinder inner diameter d_2/mm	63	81.04	80.00
Piston rod diameter d_1/mm	35	40.47	40
Damping hole 4 diameter d_z/mm	4	6.27	6.00
Damping hole 5, 7 diameter d_j/mm	4	4.52	4.50
Accumulator volume V_0/L	2.5	2.89	3.00

By comparing the original suspension (Suspension structure without any algorithm optimization) and optimized suspension (Suspension optimized by improved mopso algorithm), the comparison curves of the following three indicators are obtained in MATLAB 2020b, which are shown in Figure 14, take 1000 points evenly for each curve in the figure, and show it in Table 6 after calculating the root mean square value.

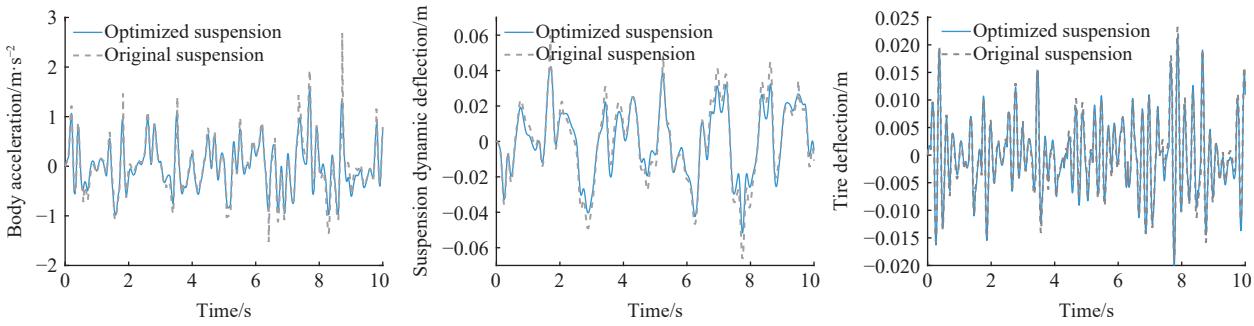

a. Body acceleration b. Suspension dynamic deflection c. Tire deflection

Figure 14 Comparison of suspension performance before and after optimization

Table 6 Root mean square and improvement rate of evaluation indicators

Evaluating indicator	Original suspension	Optimized suspension	Improvement rate
RMS of body acceleration/m·s^{-2}	0.72	0.59	18.1%
RMS of suspension dynamic deflection/m	0.023	0.019	17.4%
RMS of tire deflection/m	0.0062	0.0061	1.6%

It can be seen from Figure 14 that the body acceleration and suspension dynamic deflection of the optimized hydro-pneumatic suspension have been significantly improved. According to the analysis of Table 6, the evaluation indicators have increased by 18.1%, 17.4% and 1.6% respectively, the tire deflection has been slightly improved. In summary, the optimized structure accords with the design principle of sprayer suspension performance and effectively improves the vibration reduction performance of the sprayer.

According to the suspension characteristics, the following analysis is made: 1) the greater the vibration reduction amplitude, the greater the momentum of the hydraulic cylinder and the smaller the stiffness coefficient; 2) The stronger the ability of hydro-pneumatic suspension to resist external impact, the smaller the moving speed of hydraulic cylinder and the smaller the variation range of damping coefficient. Due to the complexity of the actual field road conditions, it is difficult to accurately analyze the suspension characteristics before and after optimization, the 0.05 m step signal simulation is used to observe the change trend of the stiffness coefficient and damping coefficient before and after the suspension optimization. It can be seen from Figure 15 that compared with before optimization, the stiffness coefficient of the optimized suspension has decreased significantly, and the damping coefficient has a smaller change range, which verifies the performance of the improved vibration reduction system from the side.

4.3 Performance verification results

After the bench test, analyze the data and select the group with the best effect among the 20 tests. The result of the 0.05 m step test is shown in Figure 16.

It can be seen from Figure 16 that the unsprung displacement of the optimized suspension is larger than that of the original suspension. In the case of the same road excitation input, the size of the unsprung displacement is determined by the momentum of the hydraulic cylinder, and is directly proportional to the momentum, and the optimized system tends to be stable faster. According to the simulation data of the suspension characteristics in Section 2.1.2, the larger the momentum, the smaller the stiffness coefficient of the system, and the test effect is consistent with the simulation; At the same time, it is found that the body displacement after the suspension optimization is smaller than that of the original suspension, and the shaking of the body is significantly reduced, which proves that the optimized hydro-pneumatic suspension system has better excitation attenuation effect.

Next, by inputting the D-level road excitation, the data received by the sensor is analyzed and processed, and the suspension performance before and after optimization is obtained and shown in Figure 17.

It can be seen from Figure 17 that the three indicators are significantly improved compared with those before optimization, which verifies the good effect of the improved algorithm, and the test results are in good agreement with the simulation results, which verifies the reliability of the simulation. Refer to the relevant data on air suspension vibration reduction of sprayer[35], by comparing the performance of the traditional air suspension of the same level sprayer with hydro-pneumatic suspension designed in this paper, and the tire deflection is converted into tire dynamic load, and the

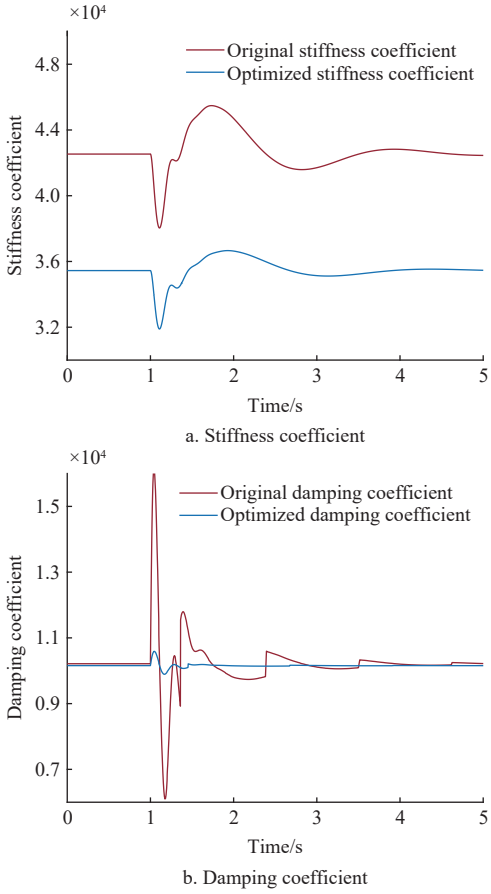

a. Stiffness coefficient

b. Damping coefficient

Figure 15 Comparison of damping coefficient and stiffness coefficient before and after optimization

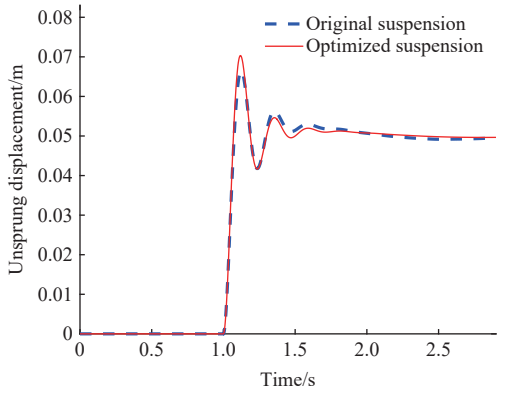

a. Unsprung displacement

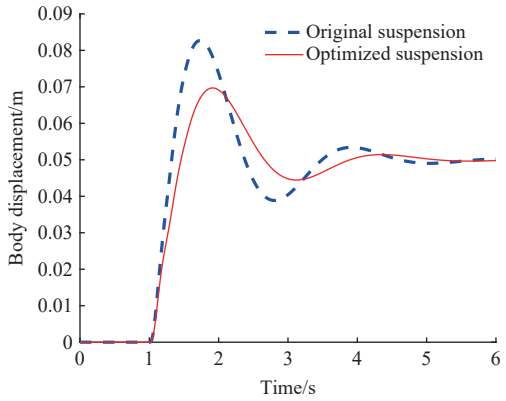

b. Body displacement

Figure 16 Comparison of step test data

comparative data of body acceleration, suspension dynamic deflection and tire dynamic load are obtained and listed in Table 7.

It can be seen from Table 7 that the hydro-pneumatic suspension chassis structure designed in this study has obvious advantages over the air suspension in terms of vibration reduction performance, which proves the rationality of the design in this paper. And the vibration reduction indicator of the hydro-pneumatic suspension optimized by the improved MOPSO algorithm has an improvement of 16.5%, 9.9% and 0.9% respectively compared with before optimization, which achieves the expected effect of multi-objective optimization, and verifies the superiority of the hydro-pneumatic suspension structure designed in this paper in the application of high clearance self-propelled sprayers, and the whole process of the optimization design method of high clearance self-propelled sprayer is completed.

5 Conclusions

This paper proposes an innovative method for the design and verification of the hydro-pneumatic suspension system of a high clearance self-propelled sprayer, which comprehensively covers the configuration design, parameter intelligent optimization, and system verification of the sprayer chassis system. The design and verification system put forward in this paper closely matches the operation characteristics of sprayer in the field. By integrating the intelligent optimization algorithm, the system systematically guides the design and test of the high clearance self-propelled sprayer.

This method is suitable for multi-level road transportation of high clearance self-propelled sprayers and complex field operation conditions. Based on the proposed configuration of the hydro-pneumatic suspension system, the suspension system optimization method of improved MOPSO algorithm based on the time-varying fusion strategy and the adaptive adjustment factor, the verification of the improved algorithm, the simulation optimization analysis of the suspension and the bench vibration test system are innovatively combined. The test results show that the optimal structure combination of the hydro-pneumatic suspension system of the sprayer can be obtained by this optimization method, the optimized hydro-pneumatic suspension system can meet the comprehensive requirements of high clearance self-propelled sprayer for ride comfort, handling stability and road friendliness. The optimized suspension performance indicator is improved by 16.5%, 9.9% and 0.9% through the bench test verification, and the vibration reduction effect is significantly improved. The verification method combining simulation and test fully proves that the sprayer hydro-pneumatic suspension optimized by the improved algorithm can take into account a variety of operating scenarios and can meet complex field operating conditions.

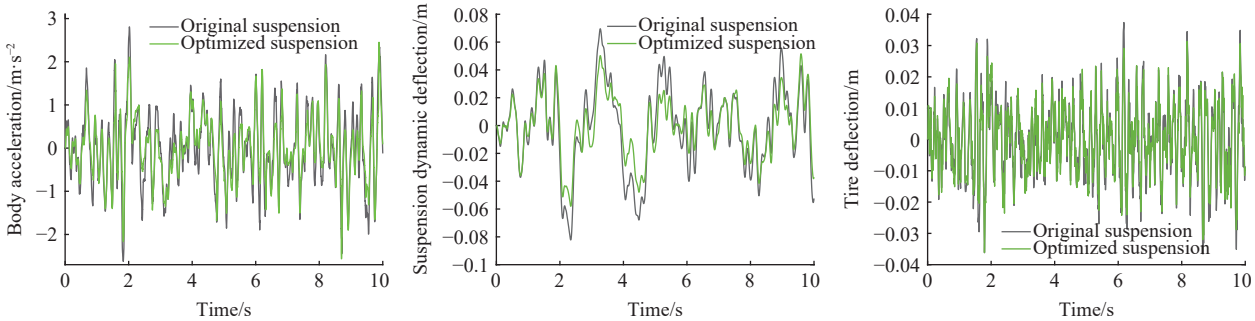

a. Body acceleration b. Suspension dynamic deflection c. Tire deflection

Figure 17 Comparison of data before and after optimization

Table 7 Comparison of test data

Evaluating indicator	Air suspension	Original hydro-pneumatic suspension	Optimized hydro-pneumatic suspension	Improvement rate/%
RMS of body acceleration/m·s^{-2}	1.56	0.97	0.81	16.5
RMS of suspension dynamic deflection/m	0.0220	0.0191	0.0172	9.9
RMS of tire dynamic load/N	4606.6	4245.06	4207.64	0.9

Therefore, the innovative method for the design of the large high clearance self-propelled sprayer vibration reduction system proposed in this paper effectively solves the problems of difficulty in improving its vibration reduction performance and poor adaptability to multiple working conditions, and provides an effective reference for the design of the vibration reduction system for the large high clearance self-propelled sprayer.

Acknowledgements

This work was financially supported by Major scientific and

Technological Innovation Projects of Shan Dong Province (Grant No.2019JZZY010728-01), supported by Bintuan Science and Technology Program (Grant No.2022DB001), and Innovative Platform of Intelligent Agricultural Equipment Design and Manufacturing (Grant No.2021XDRHXMPT29).

[References]

[1] Li W, Mao E R, Chen S Y, Li Z, Xie B, Du Y F. Design and verification of slip rate control system for straight line travel of high clearance self-propelled sprayer. Proceedings of the Institution of Mechanical Engineers, Part D: Journal of Automobile Engineering, 2022; 236(6): 1319–1335. DOI: 10.1177/09544070211032033.

[2] Sharda A, Luck J D, Fulton J P, McDonald T P, Shearer S A. Field application uniformity and accuracy of two rate control systems with automatic section capabilities on agricultural sprayers. Precision Agriculture, 2013; 14(3): 307–322.

[3] Sun W, He Y, Fu T, Wang J, Lu J, Chang J. Design and Test of Horizontal Folding Spray Boom of Sprayer. Transactions of the CSAM, 2022; 53(2): 116–127, 194. (in Chinese)

[4] Zheng J Q, Xu Y L. Development and prospect in environment-friendly pesticide sprayers. Transactions of the CSAM, 2021; 52(3): 1–16. (in Chinese)

[5] Feng J Z, Matthews C, Zheng S L, Yu F, Gao D W. Hierarchical control strategy for active hydropneumatic suspension vehicles based on genetic algorithms. Advances in Mechanical Engineering, 2015; 7(2): 951050.

[6] Zhao J K, Gu Z Q, Zhang S, Ma X K, Zhu Y F, Hu K. Research and optimization on the mechanical property of mining dump truck's hydro-pneumatic suspension. J. Mech. Eng, 2015; 51(10): 112–118.

[7] Fu Z T, Qi L J, Wang J H. Developmental tendency and strategies of precision pesticide application techniques. Transactions of the CSAM, 2007; 38(1): 189–192. (in Chinese)

[8] Chen Y, Mao E, Li W, Zhang S, Song Z, Yang S, Chen J. Design and experiment of a high-clearance self-propelled sprayer chassis. Int J Agric & Biol Eng, 2020; 13(2): 71–80.

[9] Bittner R. Suspension system for an agricultural vehicle. US, 8297634 B2, 2012; 2012-10-30.

[10] Ferreira A L, Balthazar J M, Pontes Júnior B R. Influence of suspension in the safety and comfort of a self-propelled sprayer. Engenharia Agrícola, 2010; 30(4): 753–760.

[11] Liu W, Wu C, She D. Effect of spraying direction on the exposure to handlers with hand-pumped knapsack sprayer in maize field. Ecotoxicology and Environmental Safety, 2019; 170: 107–111.

[12] Burdzik R, Konieczny Ł, Węgrzyn T. Analysis of structural and material aspects of selected elements of a hydropneumatic suspension system in a passenger car. Archives of Metallurgy and Materials, 2016; 61(1): 79–84

[13] Daou R A Z, Moreau X, Francis C. Effect of hydropneumatic components nonlinearities on the CRONE suspension. IEEE Transactions on Vehicular Technology, 2011; 61(2): 466–474.

[14] Yang C, Gao X, Liu Z, Cai L, Cheng Q, Zhang C. Modeling and analysis of the vibration characteristics of a new type of in-arm hydropneumatic suspension of a tracked vehicle. Journal of Vibroengineering, 2016; 18(7): 4627–4646.

[15] Jiao N, Guo J, Liu S. Hydro-pneumatic suspension system hybrid reliability modeling considering the temperature influence. IEEE Access, 2017; 5: 19144–19153.

[16] Solomon U, Padmanabhan C. Hydro-gas suspension system for a tracked vehicle: Modeling and analysis. Journal of Terramechanics, 2011; 48(2): 125–137.

[17] Gündoğdu Ö. Optimal seat and suspension design for a quarter car with driver model using genetic algorithms. International Journal of Industrial Ergonomics, 2007; 37(4): 327–332.

[18] Gobbi M, Mastinu G. Analytical description and optimization of the dynamic behaviour of passively suspended road vehicles. Journal of sound and vibration, 2001; 245(3): 457–481.

[19] Peng D Z, Tan G F, Fang K K, Chen L, Agyeman P K, Zhang Y X. Multiobjective optimization of an off-road vehicle suspension parameter through a genetic algorithm based on the particle swarm optimization. Mathematical Problems in Engineering, 2021; 2021(9): 1–14.

[20] Kuznetsov A, Mammadov M, Sultan I, Hajilarov E. Optimization of a quarter-car suspension model coupled with the driver biomechanical effects. Journal of Sound and Vibration, 2011; 330(12): 2937–2946.

[21] Sarker R, Ray T. An improved evolutionary algorithm for solving multi-objective crop planning models. Computers and Electronics in Agriculture, 2009; 68(2): 191–199.

[22] Farid T M, Salah A, Abbas D. Design of optimal linear suspension for quarter car with human model using genetic algorithms. Journal of Applied Sciences Research, 2011; 7(11): 1709–1720.

[23] Wu W, Hu L, Zhang Z. Collaborative optimization of nonlinear hydropneumatic suspension dynamic characteristics. Journal of Testing and Evaluation, 2020; 48(2): 20180506.

[24] Mohsen M, Kamel H, Sharaf A M, El-Demerdash S M. Optimal design of passive suspension system of a 6×6 multi-wheeled all-terrain vehicle using genetic algorithm. International Journal of Heavy Vehicle Systems, 2018; 25(3-4): 508–533.

[25] Gomes H M. A swarm optimization algorithm for optimum vehicle suspension design. In Proceedings of 20th International Congress of Mechanical Engineering, 2009; pp.1–10.

[26] Wei L, Xue T, Mao E R, Du Y F, Li Z, He X K. Design and experiment of multifunctional steering system for high clearance self-propelled sprayer. Transactions of the CSAM, 2019; 50(1): 141–151.

[27] Chen S A, Qiu F, He R, Lu S L. Analysis of self-aligning torque from vehicle kingpin inclination. Transactions of the CSAM, 2008; 39(7): 32–35. (in Chinese)

[28] Coello C, Pulido G T, Lechuga M S. Handling multiple objectives with particle swarm optimization. IEEE Transactions on Evolutionary Computation, 2004; 8(3): 256–279.

[29] Zhang Y, Tian Z, Ma W, Zhang M, Yang L. Hyperspectral detection of walnut protein contents based on improved whale optimized algorithm. Int J Agric & Biol Eng, 2022; 15(6): 235–241.

[30] Li S, Liu X, Liu Z. Interlaminar shear fatigue and damage characteristics of asphalt layer for asphalt overlay on rigid pavement. Construction and Building Materials, 2014; 68: 341–347.

[31] Sun L, Cai X, Yang J. Genetic algorithm-based optimum vehicle suspension design using minimum dynamic pavement load as a design criterion. Journal of Sound and Vibration, 2007; 301(1-2): 18–27.

[32] Czyzżak P, Jaszkiewicz A. Pareto simulated annealing-a metaheuristic technique for multiple-objective combinatorial optimization. Journal of Multi-Criteria Decision Analysis, 1998; 7(1): 34–47.

[33] Deb K, Pratap A, Agarwal S, Meyarivan T. A fast and elitist multiobjective genetic algorithm: NSGA-II. IEEE Transactions on Evolutionary Computation, 2002; 6(2): 182–197.

[34] Li K, Sha Z, Xue W, Chen X, Mao H, Tan G. A fast modeling and optimization scheme for greenhouse environmental system using proper orthogonal decomposition and multi-objective genetic algorithm. Computers and Electronics in Agriculture, 2020; 168: 105096.

[35] Chen Y. Research on design methods and characteristics of independent strut type air suspension system for high clearance sprayer. Doctoral dissertation, Beijing: China Agricultural University. 2017; pp.95–96. (in Chinese)